Tectonic velocities, dynamic topography, and relative sea level

Laurent Husson[1,2] and Clinton P. Conrad[3]

[1] A simple dynamic model based on boundary layer theory shows that dynamic topography is unlikely to vary significantly in response to short term (≤20 Myr) variations in the mean tectonic velocity. Tectonic velocities essentially mirror variations in mantle viscosity, but are not indicative of substantial modification of dynamic topography, which primarily reflects mass anomalies in the mantle. This implies that relative sea level is unlikely to be affected by "tectonic pulses" and also that observed tilting of cratonic margins cannot result from a pulse of increased tectonic velocities. Thus, relative sea level is primarily controlled by the seafloor age distribution, although long term (≥100 Myrs) changes in tectonic velocity will produce dynamic topography that reinforces sea level changes associated with changing ridge volume. **Citation:** Husson, L., and C. P. Conrad (2006), Tectonic velocities, dynamic topography, and relative sea level, *Geophys. Res. Lett.*, *33*, L18303, doi:10.1029/2006GL026834.

1. Introduction

[2] Changes in ridge volume and the seafloor age distribution were the first obvious candidates to explain relative sea level change [e.g., *Hays and Pitman*, 1973; *Kominz*, 1984], which was seen as a eustatic process [e.g., *Vail et al.*, 1977]. Because sea level is observed via flooding of continental margins, subduction-related, epeirogenic processes have also been invoked [*Mitrovica et al.*, 1989]: observed transgressions could reflect the dynamic tilting of continents above sinking slabs, and may be enhanced by faster tectonic velocities [*Gurnis*, 1990, 1993]. This reasoning, which is valid for subduction onset or cessation, has also been applied to eustatic sea level: increased negative dynamic topography above more rapidly subducting slabs may compensate, and even overcome, the effect of increased ridge volume associated with faster spreading rates [*Hager*, 1980].

[3] In order to evaluate this competition, most studies are based on semi-dynamic models where tectonic velocity is an input. Therefore, it has been argued that fast subduction stuffs dense material into the upper mantle at high rates, causing it to accumulate and generate large dynamic topography [*Gurnis*, 1990]. Such interpretations, however, do not account for the dynamic equilibrium between mantle temperature and tectonic velocities. Because slabs are thought to drive plate motions [*Conrad and Lithgow-Bertelloni*, 2004], tectonic velocities must be regarded as the result of the density contrast within the mantle and not as its cause. Thus, plate and slab velocities must be consistent with (i) their intrinsic buoyancy and (ii) the density and viscosity of the mantle, as they are in several dynamically-consistent studies [e.g., *Mitrovica et al.*, 1989; *Ricard and Vigny*, 1989] (we discard dynamic fluctuations in upwellings as a control on plate dynamics below). These interactions can be captured by a simple, yet dynamically consistent, analysis based on steady-state boundary layer theory that evaluates the competition between seafloor age distribution and dynamic topography.

2. Dynamic Topography in a Convective System

[4] Dynamic topography is the vertical component of the response of an interface, like the surface of the Earth, to the viscous flow of the underlying fluid. In a highly viscous system like the mantle, inertia is negligible and dynamic topography is independent of viscosity for a uniform Newtonian fluid [*Morgan*, 1965]. Therefore the dynamic volume of the deflected Earth surface can be reduced to an integral function of the mass heterogeneities in the Earth's mantle. Note that support of slabs by a high-viscosity lower mantle may decrease dynamic topography amplitudes at the surface [*Hager*, 1984]. Thus, our use of a mantle of uniform viscosity leads to upper bounds on dynamic volumes in the analysis below. In a chemically uniform convective system, density heterogeneities only depend on the thermal state of the mantle. In such a case, the key parameter affecting dynamic topography is the temperature of the mantle, which sets the magnitude of the density contrast and the volume of these density heterogeneities (i.e., the volume of the slab).

2.1. Plate Velocity and Boundary Layer Theory

[5] Boundary layer theory satisfactorily explains the structure and kinematics of a convecting Earth (see *Bercovici et al.* [2000] for a review). The buoyancy force F_B that drives the subduction is balanced by the drag forces F_{D_h} and F_{D_v} that act on the horizontal and vertical boundaries of the convection cell. Following the derivation of [*Turcotte and Schubert*, 2002], the forces per unit length are:

$$F_B = \rho_0 \alpha T_m g b \frac{\overline{u}}{\overline{v}} \left(\frac{\kappa \lambda}{\pi \overline{u}}\right)^{1/2},$$

$$F_{D_h} = 2\mu a \overline{u}; F_{D_v} = 2\frac{\mu}{a}\overline{v}. \tag{1}$$
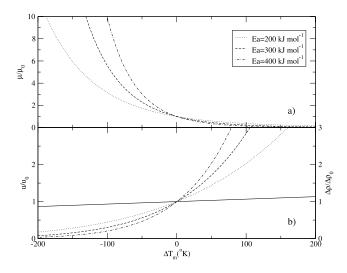
$\rho_0 \alpha T_m / 2$ is the mean density contrast within the mantle, ρ_0 is the reference density for the mantle, α is the coefficient of thermal expansion, T_m the temperature increase in the mantle ($T_m/2$ is the temperature in the core of the convective mantle assuming a symmetric temperature profile), and κ is

[1]Massachusetts Institute of Technology, Cambridge, Massachusetts, USA.
[2]Now at Géosciences Rennes, UMR CNRS 6118, Université de Rennes 1, Campus de Beaulieu, Rennes, France.
[3]Department of Earth and Planetary Sciences, Johns Hopkins University, Baltimore, Maryland, USA.

Figure 1. (a) Mantle viscosity variation as a function of changes in mantle temperature, ΔT_m; (b) Variations in the density contrast $\delta\rho$ through the mantle (right axis, solid line) and viscosity (left axis, broken lines) as a function of mean temperature variation in the mantle. Calculations are performed for different activation energies. Reference values are taken for present day ($T_{m0} = 3000K$, $u_0 = 3.1$ cm yr^{-1}, $b = 2800$ km, $\alpha = 3 \times 10^{-5}$ K^{-1}, $\rho_a = 3250$ kg m^{-3}), and an aspect ratio $a = 1$.

the thermal diffusivity. a is the mean aspect ratio of the convection cell, i.e. the ratio of its width λ over its thickness b, g is the acceleration of gravity, $\bar{u}$ is the average velocity of the upper and lower boundary layers, and $\bar{v}$ is the vertical velocity of these layers after foundering.

[6] A force balance leads to a relation between $\bar{u}$ and the Rayleigh number Ra:

$$\bar{u} = \frac{\kappa}{b} \frac{a^{7/3}}{(1 + a^4)^{2/3}} \left(\frac{Ra}{2\sqrt{\pi}} \right)^{2/3} \qquad (2)$$

where $Ra = \frac{\rho_0 \alpha T_m g b^3}{\mu \kappa}$. Note that this relation becomes flawed for stiff lithospheres ($\sim 10^{23}$ Pa s [Conrad and Hager, 1999]).

2.2. Average Mantle Temperature

[7] The temperature-dependent viscosity μ is given by

$$\mu = \mu_0 \exp\left[\frac{E_a}{RT_m/2} - \frac{E_a}{RT_{m0}/2} \right], \qquad (3)$$

where E_a is the activation energy of olivine, R is the gas constant, and μ_0 is the viscosity at the reference average temperature $T_{m0}/2$. Although T_m is the only free parameter, μ is extremely sensitive to T_m due to the exponential nature of their relationship (Figure 1a). By combining equations 2 and 3 and setting $a = 1$, we write:

$$\bar{u} = \kappa^{1/3} b \left[\frac{\rho_0 \alpha T_m g}{4\sqrt{\pi}\mu_0 \exp\left(\frac{E_a}{RT_m/2} - \frac{E_a}{RT_{m0}/2} \right)} \right]^{2/3}. \qquad (4)$$
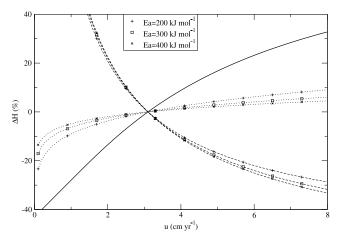
Any variation in the vigor of the convection (as measured by Ra) should be mirrored by a variation in $\bar{u}$ (equation 2). Conversely, any observed variation in $\bar{u}$ implies a variation in T_m, which is the only free parameter in Ra. Equation 4

allows us to relate plate velocity variations to departures ΔT_m from the current mantle temperature (Figure 1b). Our choice of $\mu_0 = 6.1 \times 10^{22}$ Pa s is based on inferred present-day values for a whole mantle convection scheme (see reference values in Figure 1), and is in the range of independent estimates [Lambeck and Chappell, 2001; Mitrovica and Forte, 2004]. Possible values for E_a for diffusion creep of olivine range from ~ 200 to more than 400 kJ/mol [Hirth and Kohlstedt, 1995, 2003; Korenaga and Jordan, 2002], leading to a large uncertainty in μ due to its position in the exponential (Figure 1a). Because viscosity depends exponentially on E_a, it influences velocity significantly. An increase in T_m by ~ 45 K is needed to double the value of $\bar{u}$ with $E_a = 400$ kJ mol^{-1} whereas as much as ~ 100K is needed with $E_a = 200$ kJ mol^{-1} (Figure 1b).
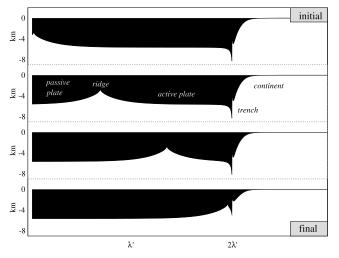
[8] Because it depends exponentially on T_m, viscosity can vary by one to two orders of magnitude for reasonable changes in T_m (Figure 1a), while the density contrast increases by only $\sim 6.5\%$ per 100K temperature increase (Figure 1b). This implies that any changes to Ra are dominated by viscosity, not density, variations.

2.3. Dynamic Volume

[9] To first order, dynamic topography H is a linear function of the mass anomalies at depth. For a subduction zone, slab mass can be expressed as a function of slab volume and density contrast $\rho_0 \alpha T_m/2$. Both quantities may change with time due to changes in plate velocity (4) or the aspect ratio of the convective cell (2). According to (2) an increase in aspect ratio ($a > 1$) leads to a decrease in Ra, and thus a decrease in T_m for constant $\bar{u}$. However, the decrease in T_m is a maximum of 25K and modifies dynamic topography by only 3%. A decrease in aspect ratio, while leading to a larger T_m increase, is unphysical for the Earth.

Figure 2. Relative variations of the dynamic volume as a function of mean plate velocity for an instantaneous (short-lived) departure from the 3.1 cm yr^{-1} reference tectonic velocity (dotted lines) and a change to a new steady state velocity (dashed lines). The variation in the volume of a half-ridge is shown for comparison (solid line). Note that changes in the absolute ridge volume are generally 1.5 to 6 times larger than instantaneous changes in the absolute dynamic volume. E_a is the activation energy, other parameters are as in Figure 1.

Figure 3. Evolution of the modeled morphologies (here calculated for $\bar{u}$ = 3.1 cm/yr). Trench morphology is dynamic, see text for details.

[10] Instantaneous variations in tectonic velocity do not affect the volume of subducted material, and thus cause only small (5–7%) changes in dynamic topography associated with the inferred change in T_m (Figure 2, dotted lines). Long-term variations in velocity may arise, for instance because of the blanketing effect of continents [e.g., *Trubitsyn et al.*, 2003], and should lead to thinner slabs because plates are younger when they subduct. In steady state [see *Turcotte and Schubert*, 2002], the thickness of the boundary layer δ varies as

$$\delta = 1.7 \frac{b}{Ra^{1/3}}. \qquad (5)$$

The volume of the slab is its length times its thickness. Thus assuming similarity between the thickness of the conductive and the mechanical layers, the volume also varies as $Ra^{-1/3}$. Dynamic topography is expected to vary linearly with the volume of the slab, and therefore with its thickness δ. We evaluate δ as a function of $\bar{u}$ (or T_m) from equation 2 and 5 and get

$$\delta = \frac{1.7}{(2\sqrt{\pi})^{1/3}} \left(\frac{b\kappa}{\bar{u}} \right)^{1/2}, \qquad (6)$$

which shows that δ varies as $u^{-1/2}$. Figure 2 (dashed lines) shows the relative variation of dynamic topography accounting for both density and plate thickness variations consistent with a long-term change in average plate velocity. The effect of plate thickness variations opposes and overcomes that of density variations; it can modify the dynamic volume by ±25% for a reasonable range of velocities.
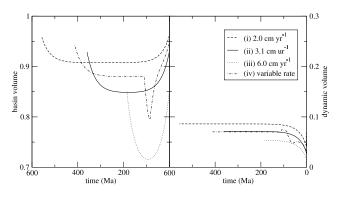
[11] Long-term thermal disturbances are expected to accompany the Wilson cycle and should obey (6). Unfortunately, we do not have access to plate velocities over an entire cycle to verify this correlation. However, if the above relationship is correct, the dynamic volume would be smaller during periods of a warmer mantle characteristic

of a supercontinental setting compared to times after continental breakup, when temperatures (and presumably tectonic velocities) are lower.

3. Examples

3.1. The Model

[12] Following the formulation of section 2, we constructed an idealized system that incorporates a spreading ridge moving toward a subduction zone (somewhat akin to the Mesozoic-Cenozoic disappearance of the Farallon plate). The modeled section is one period of an idealized periodic Earth-like system. In order to keep a surface balance for the model, plate formation is balanced by plate destruction. This implies that subduction rates and trench migration rates are linear functions of spreading rates. The basin volume above the ridge is calculated from the age-depth relationship of cooling seafloor [after *Stein and Stein*, 1992]. The dynamic volume above the subducting slab is calculated for a sine-shaped thin sheet slab sinking to a depth of 670 km with a half-wavelength of 500 km (slabs in the lower mantle are neglected). The slab is discretized into horizontal mass lines (or linear *Stokeslets*) sinking vertically; the total Stokes flow is given by the sum of the elementary *Stokeslets* [*Morgan*, 1965; *Batchelor*, 1967; *Davies*, 1981; *Harper*, 1984; *Husson*, 2006]. Stresses normal to the surface are calculated using the "image" technique [*Morgan*, 1965], which accounts for the presence of the surface interface. The buoyancy of the subducting material is computed from the age of the oceanic lithosphere at the time it subducts, and compared to the density of the asthenosphere, as calculated in section 2.

[13] Although not readily applicable to Earth's history, the following examples encompass most possible scenarii. The reference tectonic velocity is set to $\bar{u}$ = 3.1 cm yr^{-1} (mean present-day half-spreading rates, *Cogné and Humler* [2004]), from which T_{m0}, μ_0 and δ are calculated. The initial state (Figure 3, top) is set to an end-member situation, where the entire ocean consists of a plate of length $2\lambda'$ subducting beneath a continent of length λ'. The length

Figure 4. Changes in ridge volume associated with (a) the evolving age distribution of the seafloor and (b) changes in the dynamic volume associated with changes in subduction-induced dynamic topography. In each case, the volume is given as a fraction of the total volume of the ocean basin relative to the initial volume (basin volume + dynamic volume) of the reference case (Figure 3, top). Here 0 Ma (present-day) is the final state.

scale λ' is the plate length produced in 180 myrs at $u_0 = 3.1$ cm yr^{-1} (5580 km). The ridge spreads and migrates toward the subduction zone, causing the subducting plate to shrink at the expense of a passive oceanic plate, which grows with time (Figure 3). In the final state (Figure 3, bottom), the ridge meets the trench, leaving only a single oceanic plate spanning the expanse of the ocean.

3.2. Ridge Volume Versus Dynamic Volume

[14] Let us first consider changes in the volume of the ocean basin due to age-related changes in bathymetry. For steady tectonic velocities (Figure 4, $\bar{u} = 2.0$ cm/yr (i), $\bar{u} = 3.1$ cm/yr (ii, reference) and $\bar{u} = 6.0$ cm/yr (iii)), we modify plate thickness according to (6) and measure changes in basin volume by calculating changes in ridge volume (Figure 4a). In each case, basin volume initially decreases due to the replacement of old subducting lithosphere with young seafloor created at the ridge. As the calculation nears the present-day (0 Ma), basin volume increases again as destruction of young seafloor increases the average seafloor age. The total variation in basin volume for a given spreading rate ranges between 6% and 19% depending on the rate (Figure 4a). Lower rates show larger basin volumes and smaller variations in basin volume because the average seafloor age is older and therefore less variable. The minima in basin volume vary by 8–15% compared to the reference case.

[15] The dynamic volume associated with deflection of the seafloor by subduction-induced downwelling also varies with time as the ridge moves toward the trench (Figure 4b). However, most of the variation occurs only within the last ~50 Myr as the ridge nears the trench. This process causes increasingly younger material to be subducted, which decreases mantle densities associated with subduction and thus the dynamic topography as well (although not completely to zero because some slab is still present when the ridge meets the trench). The total variation in volume is always less than 10% of the total volume, significantly smaller than the volume changes associated with changes in the seafloor age distribution. Expected variations in plate rates produce at most only a 3% variation in total volume at any given time (Figure 4b).

3.3. Variable Plate Rates

[16] The impact of a tectonic pulse on dynamic volume can be addressed by considering the controversial [*Heller et al.*, 1996; *Cogné and Humler*, 2004] end-member situation proposed by *Hays and Pitman* [1973] for changes in Cretaceous tectonic velocities: we assign 2.5 cm yr^{-1} before 110 Ma, 6.5 cm yr^{-1} between 110 and 85 Ma, 2.24 cm yr^{-1} between 85 and 10 Ma, and 3.1 cm yr^{-1} for the last 10 Ma. Again, the mean seafloor age controls the first-order basin volume and increased spreading rates generate a significant eustatic perturbation of about 10% of basin volume after only a few *myrs* (Figure 4a). However, because the pulse is relatively short lived, the volume of subducted material remains nearly constant through time and only the mantle density contrast varies. As a result, changes in dynamic topography are minor (Figure 4b): dynamic topography increases slightly (about 1% of total basin volume) during the tectonic pulse due to the more rapid placement of oceanic lithosphere into the mantle. The larger decrease in dynamic volume that follows (70 to 50 Ma) represents subduction of the more buoyant lithosphere generated during the pulse.

4. Discussion

[17] Instantaneous (short-lived) variations in plate velocity only increase the dynamic volume by at most ±5–7% because fluctuations in plate velocity are primarily due to changes in viscosity rather than density. In terms of volumes, the dynamic topography that we evaluate from the Stokeslets approximation [e.g., *Harper*, 1984; *Husson*, 2006] above a subducting slab is typically ~2.4 × 10^9 m^3 per m of subduction zone. This yields a maximum variation of 0.17 × 10^9 m^3 per unit length associated with a change in tectonic velocity. If all upper plates flooded simultaneously, such a variation, integrated over the 43500 km of present-day trench length and distributed over the surface of the ocean, would induce a 22 m variation in relative sea level. Such amplitudes are unlikely to be recorded by the geological record. We conclude that short-term variations in relative sea level are most reflective of changes to the seafloor age distribution, as emphasized by *Heller and Angevine* [1985] and *Heller et al.* [1996] and constrained by *Xu et al.* [2006].

[18] Long-lived increases in tectonic velocities decrease the volume of subducted material, and thus lead to larger fluctuations in dynamic topography than can be expected from short-term variations. Variations of up to ±25% of the dynamic volume (but only about 3% of the basin volume) can be expected. Following the above calculation, 25% variations of the dynamic volume indicate volume changes of 0.61 × 10^9 m^3 per m of trench, and would generate a 78 m high variation in relative sea level. Note that this process reinforces the accompanying variations of ridge volume with plate velocity (Figure 4a) and in no case does it compensate them. By comparison, the volume of a half-ridge with a half-spreading rate of 3.1 cm yr^{-1} is about 3 × 10^9 m^3 per m of ridge length [following *Stein and Stein*, 1992]. This volume varies efficiently with plate velocities and it can bulge up by 25% while doubling the plate velocity (Figure 2, solid line), inducing volume variations of about 0.75 × 10^9 m^3 per unit length. For long-term tectonic changes, dynamic topography reinforces trends associated with seafloor rejuvenation caused by continental breakup or increased tectonic velocities. Both processes are comparable in magnitude and can certainly be recorded in the Earth's long term history.

[19] Another consequence of dynamic topography is the tilt of continental margins. *Gurnis* [1990, 1993] suggested that increased dynamic topography and epeirogenic processes on the margin of continents would accompany a tectonic pulse; the present model suggests that this effect is minor because tectonic velocity reflects mantle temperature more strongly than the buoyancy contrast between the slab and the mantle. The tilt of a margin can be modified only when the buoyancy of the slab is modified, typically during subduction initiation or cessation, or in the event of slab detachment [*Buiter et al.*, 2002; *Mitrovica et al.*, 1989].

References

Batchelor, G. (1967), *An Introduction to Fluid Mechanics*, Cambridge Univ. Press, New York.

Bercovici, D., Y. Ricard, and M. Richards (2000), The relation between mantle dynamics and plate tectonics: A primer, in *The History and Dynamics of Global Plate Motions*, *Geophys. Monogr. Ser.*, vol. 121, edited by R. G. M. A. Richards and R. van der Hilst, pp. 5–46, AGU, Washington, D. C.

Buiter, S. J. H., R. Govers, and M. J. R. Wortel (2002), Two-dimensional simulations of surface deformation caused by slab detachment, *Tectonophysics*, *394*, 195–210.

Cogné, J. P., and E. Humler (2004), Temporal variation of oceanic spreading and crustal production rates during the last 180 my, *Earth Planet. Sci. Lett.*, *227*, 427–439.

Conrad, C. P., and B. H. Hager (1999), The thermal evolution of an Earth with strong subduction zones, *Geophys. Res. Lett.*, *26*, 3041–3044.

Conrad, C. P., and C. Lithgow-Bertelloni (2004), The temporal evolution of plate driving forces: Importance of "slab suction" versus "slab pull" during the Cenozoic, *J. Geophys. Res.*, *109*, B10407, doi:10.1029/2004JB002991.

Davies, G. F. (1981), Regional compensation of subducted lithosphere: Effects on geoid, gravity and topography from a preliminary model, *Earth Planet. Sci. Lett.*, *54*, 431–441.

Gurnis, M. (1990), Ridge spreading, subduction, and sea-level fluctuations, *Science*, *250*, 970–972.

Gurnis, M. (1993), Phanerozoic marine inundation of continents driven by dynamic topography above subducting slabs, *Nature*, *364*, 589–593.

Hager, B. (1980), Eustatic sea level and spreading rate are not simply related, *Eos Trans. AGU*, *61*, 374.

Hager, B. H. (1984), Subducted slabs and the geoid: Constraints on mantle rheology and flow, *J. Geophys. Res.*, *89*, 6003–6015.

Harper, J. F. (1984), Mantle flow due to internal vertical forces, *Phys. Earth Planet. Inter.*, *36*, 285–290.

Hays, J., and W. Pitman (1973), Lithospheric plate motion, sea level changes and climatic and ecological consequences, *Nature*, *246*, 18–22.

Heller, P. L., and C. L. Angevine (1985), Sea-level cycles during the growth of Atlantic-type oceans, *Earth Planet. Sci. Lett.*, *75*, 417–426.

Heller, P. L., D. L. Anderson, and C. L. Angevine (1996), Is the middle Cretaceous pulse of rapid sea-floor spreading real or necessary?, *Geology*, *24*, 491–494.

Hirth, G., and D. Kohlstedt (1995), Experimental constraints on the dynamics of the partially molten upper-mantle: Deformation in the diffusion creep regime, *J. Geophys. Res.*, *100*, 1981–2001.

Hirth, G., and D. Kohlstedt (2003), Rheology of the upper mantle wedge: A view from the experimentalists, in *Inside the Subduction Factory*, *Geophys. Monogr. Ser.*, vol. 138, edited by J. Eiler and M. Hirschmann, pp. 83–104, AGU, Washington, D. C.

Husson, L. (2006), Dynamic topography above retreating subduction zones, *Geology*, *34*(9), 741–744, doi:10.1130/G22436.

Kominz, M. (1984), Oceanic ridge volume and sea-level change—An error analysis, in *Interregional Unconformities and Hydrocarbon Accumulation*, *Mem. Ser.*, vol. 36, edited by J. Schlee, pp. 109–127, Am. Assoc. of Petrol. Geol., Tulsa, Okla.

Korenaga, J., and T. H. Jordan (2002), On "steady-state" heat flow and the rheology of oceanic mantle, *Geophys. Res. Lett.*, *29*(22), 2056, doi:10.1029/2002GL016085.

Lambeck, K., and J. Chappell (2001), Sea level change through the last glacial cycle, *Science*, *292*, 679–686.

Mitrovica, J. X., and A. M. Forte (2004), A new inference of mantle viscosity based upon joint inversion of convection and glacial isostatic adjustment data, *Earth Planet. Sci. Lett.*, *225*, 177–189.

Mitrovica, J., C. Beaumont, and G. Jarvis (1989), Tilting of continental interiors by the dynamical effects of subduction, *Tectonics*, *8*, 1079–1094.

Morgan, W. (1965), Gravity anomalies and convection currents, *J. Geophys. Res.*, *70*, 6175–6187.

Ricard, Y., and C. Vigny (1989), Mantle dynamics with induced plate tectonics, *J. Geophys. Res.*, *94*, 17,543–17,559.

Stein, C. A., and S. Stein (1992), A model for the global variation in oceanic depth and heat flow with lithospheric age, *Nature*, *359*, 123–129.

Trubitsyn, V. P., W. D. Mooney, and D. H. Abbott (2003), Cold cratonic roots and thermal blankets: How continents affect mantle convection, *Int. Geol. Rev.*, *45*, 479–496.

Turcotte, D., and G. Schubert (2002), *Geodynamics*, Cambridge Univ. Press, New York.

Vail, P., R. Mitchum, R. Todd, J. Widmier, S. Thompson, J. Sangree, J. Bubb, and W. Hatelid (1977), *Seismic Stratigraphy and Global Changes of Sea Level: Seismic Stratigraphy—Applications to Hydrocarbon Exploration*, pp. 49–212, Am. Assoc. of Petrol. Geol., Tulsa, Okla.

Xu, X. Q., C. Lithgow-Bertelloni, and C. P. Conrad (2006), Global reconstructions of cenozoic seafloor ages: Implications for bathymetry and sea level, *Earth Planet. Sci. Lett.*, *243*, 552–564.

————————

C. P. Conrad, Department of Earth and Planetary Sciences, Johns Hopkins University, Baltimore, MD 21218, USA. (conrad@jhu.edu)

L. Husson, Géosciences Rennes, UMR CNRS 6118, Université de Rennes 1, Campus de Beaulieu, F-35042 Rennes, France. (lhusson@mit.edu)